Complex transient dynamics of hidden attractors in a simple 4D system*

Dang Xiao-Yu(党小宇)[a], Li Chun-Biao(李春彪)[b], Bao Bo-Cheng(包伯成)[c]†, and Wu Hua-Gan(武花干)[d]

[a] College of Electronic and Information Engineering, Nanjing University of Aeronautics and Astronautics, Nanjing 210016, China
[b] School of Electronic & Information Engineering, Nanjing University of Information Science & Technology, Nanjing 210044, China
[c] School of Information Science and Engineering, Changzhou University, Changzhou 213164, China
[d] School of Electronic and Optical Engineering, Nanjing University of Science and Technology, Nanjing 210094, China

(Received 10 October 2014; revised manuscript received 21 December 2014; published online 27 March 2015)

A simple four-dimensional system with only one control parameter is proposed in this paper. The novel system has a line or no equilibrium for the global control parameter and exhibits complex transient transition behaviors of hyperchaotic attractors, periodic orbits, and unstable sinks. Especially, for the nonzero-valued control parameter, there exists no equilibrium in the proposed system, leading to the formation of various hidden attractors with complex transient dynamics. The research results indicate that the dynamics of the system shows weak chaotic robustness and depends greatly on the initial states.

Keywords: transient dynamics, hidden attractor, equilibrium

PACS: 05.45.−a, 05.45.Ac, 05.45.Pq **DOI:** 10.1088/1674-1056/24/5/050503

1. Introduction

Due to existing hidden attractors, some particular dynamical systems related to line equilibrium or without equilibrium or stable equilibrium have received much attention in recent years.[1–9] For the classical chaotic systems including the Lorenz system,[10] Chua's circuit,[11] and many other widely-known systems,[12–15] their attractors, called self-excited attractors, emerge from the corresponding unstable equilibria with index 2, i.e., an attractor with a basin of attraction is associated with an unstable equilibrium. However, for these particular chaotic systems, their attractors are hidden because the generations have nothing to do with any unstable equilibrium and there is no way to choose an initial condition that guarantees that they will be found.[5,6] A hidden attractor with a small basin of attraction is not associated with an unstable equilibrium,[1,4] which is of considerable importance in engineering applications because of the occurrence of unexpected behaviors in some real nonlinear dynamical systems,[16–19] such as Chua's electrical circuit,[16,17] the drilling system actuated by an induction motor with a wound rotor,[18] the aircraft flight control system with input saturation,[19] and so on.

Like the self-excited attractors, the hidden attractors have many similar dynamical behaviors, including chaos, bifurcation, periodic window, coexisting attractors, etc.[1,16] Some complex transient transition behaviors of the hidden attractors are rarely reported in the literature. In this paper, a simple four-dimensional (4D) system with seven terms, two quadratic nonlinearities, and one control parameter are considered, which is based on an extension of the three-dimensional (3D) robust chaotic system in Ref. [13]. The proposed system has a line equilibrium for the zero-valued control parameter or no equilibrium for the nonzero-valued control parameter. In fact, the triggering dynamics closely depends on the initial states for the system with a line equilibrium[4,15] and the generating attractors are all hidden for the system without any equilibrium.[1,3,7–9] Thus, based on the above two cases, the dynamical behaviors of the proposed system will be investigated in detail in this paper.

2. New chaotic system with line equilibrium or without equilibrium

By simplifying a three-dimensional robust chaotic system in Ref. [13] and using a linear feedback controller, a simple 4D system is proposed and expressed as

$$\begin{cases} \dot{x} = y - x, \\ \dot{y} = xz + \mu, \\ \dot{z} = -xy + w, \\ \dot{w} = x, \end{cases} \tag{1}$$

where μ is a unique control parameter.

The system is dissipative. The dissipativity can be derived from

$$\nabla V = \frac{\partial \dot{x}}{\partial x} + \frac{\partial \dot{y}}{\partial y} + \frac{\partial \dot{z}}{\partial z} + \frac{\partial \dot{w}}{\partial w} = -1. \tag{2}$$

Thus, system (1) is dissipative with solutions as time goes to infinity that contract onto an attractor of zero measure in 4D state space.

*Project supported by the National Natural Science Foundation of China (Grant No. 51277017), the Natural Science Foundation of Jiangsu Province, China (Grant No. BK2012583), and the Fundamental Research Funds for the Central Universities of China (Grant No. NS2014038).

†Corresponding author. E-mail: mervinbao@126.com

© 2015 Chinese Physical Society and IOP Publishing Ltd

By setting the left-hand side to zero, we have

$$\begin{cases} y-x=0, \\ xz+\mu=0, \\ -xy+w=0, \\ x=0. \end{cases} \tag{3}$$

It is found that there are two cases for the solutions of Eq. (3).

Case 1 When $\mu=0$, system (1) has an equilibrium set

$$E=\{(x,y,z,w)\,|x=y=w=0,z=c\}, \tag{4}$$

where c is uncertain but constant, corresponding to the z axis. Thus, the equilibrium set E is also known as a line equilibrium.[4,15]

Case 2 When $\mu\neq 0$, equation (3) has no real solutions and system (1) has no equilibrium, implying that when μ is nonzero, the generating attractors of the system are all hidden with the basin of attraction not intersecting with the small neighborhood of any equilibrium.[1,3,7–9] Furthermore, the terms on the left-hand side of Eq. (3) must be zero after the time average so that the attractors can be bounded.[1]

For Case 1, the Jacobian matrix at the equilibrium set E is obtained as

$$\boldsymbol{J}=\begin{bmatrix} -1 & 1 & 0 & 0 \\ c & 0 & 0 & 0 \\ 0 & 0 & 0 & 1 \\ 1 & 0 & 0 & 0 \end{bmatrix}. \tag{5}$$

The characteristic polynomial is derived as

$$\det(\mathbf{1}\lambda-\boldsymbol{J})=\lambda^2(\lambda^2+\lambda-c)=0. \tag{6}$$

Solving Eq. (6) yields

$$\lambda_1=0.5(\sqrt{1+4c}-1),\ \ \lambda_{2,3}=0,\ \ \lambda_4=-0.5(\sqrt{1+4c}+1). \tag{7}$$

It is found that when $c>0$ and $\lambda_1>0$, i.e., the equilibrium set E is an unstable saddle point, otherwise the equilibrium set E is a stable saddle point or a stable saddle focus. The resulting eigenvalues show that the stability of the equilibrium set E has a close relationship with the initial states, leading to the dependent dynamics of system (1) associated with the initial states.[4,15]

3. Transient hyperchaotic attractors and unstable sinks

Firstly, we consider Case 1 of $\mu=0$ or system (1) with a line equilibrium. The parameter $z(0)$ in the initial states (0, 0.000001, $z(0)$, 0) is taken as a varying parameter. With the variation of $z(0)=c$, the Lyapunov exponent spectra at $t=2$ ks and the corresponding bifurcation diagram in the time interval [200, 400] s are depicted in Figs. 1(a) and 1(b), respectively. Here, the four Lyapunov exponents are denoted by LE_i ($i=1, 2, 3, 4$), with $\mathrm{LE}_1>\mathrm{LE}_2>\mathrm{LE}_3>\mathrm{LE}_4$. For clarity, the largest three Lyapunov exponents LE_1, LE_2, and LE_3 are presented, whereas the fourth Lyapunov exponent LE_4 is omitted because its value with a large negative is independent of the system dynamics. As the initial state $z(0)=c$ gradually increases, system (1) starts from stable sinks with the zero largest Lyapunov exponent, and then enters the complex dynamics of transient hyperchaotic attractors or steady chaotic attractors, and unstable sinks appear alternately. Thus, the system (1) is interestingly multistable[20] and can exhibit complicated nonlinear phenomena, leading to extreme dependence of the devolvement of phase trajectories on the initial states.[15]

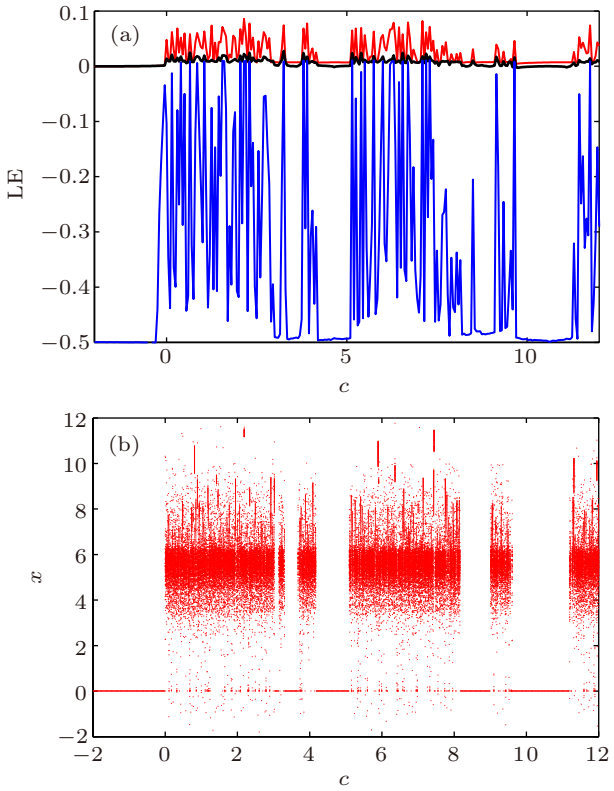


Fig. 1. (color online) Dynamics with the variation of $z(0)=c$: (a) the largest three Lyapunov exponents; (b) bifurcation diagram of the state variable x.

The above two examples illustrate that the hyperchaotic attractors in system (1) are transient. When $c=0$, the equilibrium set E of system (1) is only an origin and the corresponding four eigenvalues are $\lambda_1=0$, $\lambda_{2,3}=0$, and $\lambda_4=-1$, implying that the origin is a critical point with uncertain stability. The phase portrait in the x–y plane, the time-domain waveform of the variable z, and the largest three Lyapunov exponents for $c=0$ are shown in Figs. 2(a), 2(b), and 2(c), respectively. Figure 2(a) displays the phase portrait in a limited time interval. Figure 2(b) illustrates that the dynamics of system (1) has a transition from the origin to transient hyperchaotic behaviors, and to unstable sinks. Figure 2(c) exhibits that there are two positive Lyapunov exponents LE_1 and LE_2 in a limited time interval and the largest Lyapunov exponent

tends to be zero with time evolution, resulting in the transient hyperchaos in system (1).

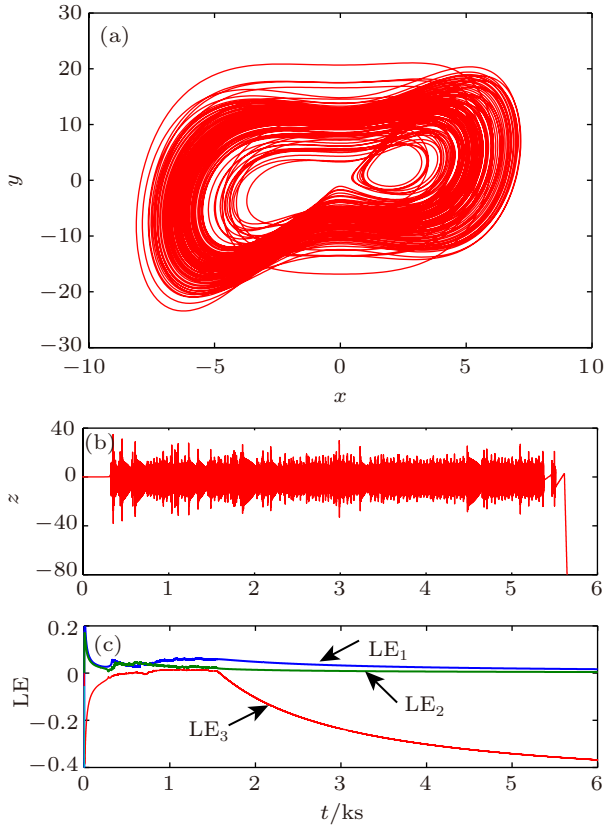


Fig. 2. (color online) Transient hyperchaotic attractors for $c = 0$. (a) Phase portrait in the time interval [2.2, 2.5] ks. (b) Time-domain waveform of the state variable z. (c) The largest three Lyapunov exponents versus time.

When $c = 6$, the equilibrium set E of system (1) is a nonzero equilibrium and the four eigenvalues are calculated by Eq. (7) as $\lambda_1 = 2$, $\lambda_{2,3} = 0$, and $\lambda_4 = -3$, which means that the nonzero equilibrium is an unstable saddle. Correspondingly, the four Lyapunov exponents are (0.0566, 0.0176, 0.0091, −1.0834) at $t = 2$ ks and (0.0181, 0.0039, −0.3609, −0.6621) at $t = 10$ ks. These results show that the system (1) is transient hyperchaotic and has a transition from transient hyperchaotic to chaotic behaviors with the long time evolution. More examples of complex transient dynamical behaviors can be demonstrated by numerical simulation under different initial states of the state variable z.

Specially, the sinks with the largest zero Lyapunov exponent in the region of $c < -0.02$ are stable, implying that all trajectories of the state variable z are convergent to a stable point with the time evolution; whereas the sinks with a positive largest Lyapunov exponent and a zero Lyapunov exponent in the region of $c > 0$ are unstable, where with the time evolution, three trajectories of the state variables x, y, and w are convergent to a stable point and the trajectory of the state variable z tends to be infinite. An example for the unstable sink is plotted in Fig. 3, where the initial state $c = 10$ and the four Lyapunov exponents are (0.0059, −0.001, −0.4945, −0.5103) at $t = 2$ ks.

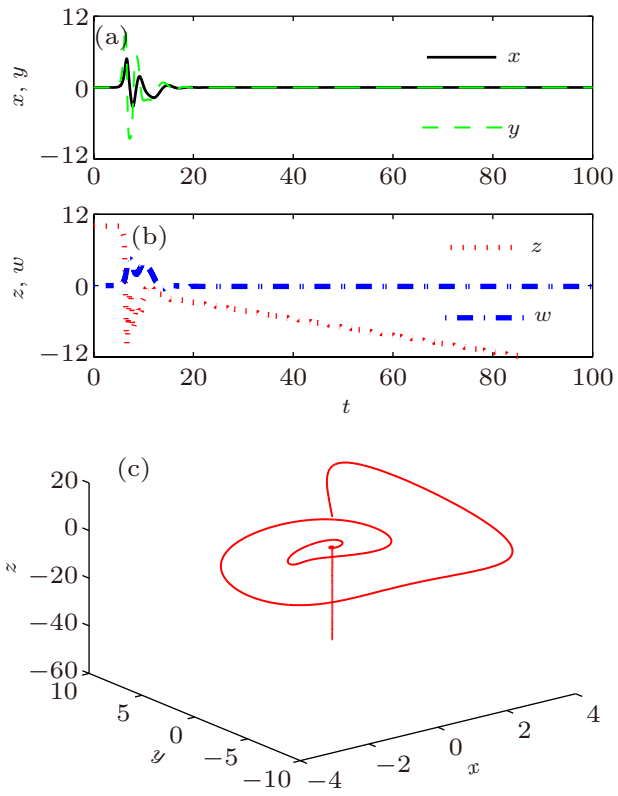


Fig. 3. (color online) Unstable sinks, where the trajectory of z tends to be infinite with the time evolution: (a), (b) time-domain waveforms of four state variables; (c) corresponding trajectory in the x–y–z space.

4. Hidden attractors with complex transient behaviors

Now we consider Case 2 of $\mu \neq 0$ or system (1) without equilibrium. The initial states of system (1) are selected as (1, 1, 1, 1) and the control parameter μ is regarded as a varying parameter. The largest three Lyapunov exponents at $t = 2$ ks and the corresponding bifurcation diagram in the time interval [200, 400] s are displayed in Figs. 4(a) and 4(b), respectively. When μ gradually increases, system (1) starts from transient hyperchaotic behaviors and then degrades into chaotic behaviors, and finally settles down periodic behaviors at $\mu = 5.7$. Two typical phase portraits within the transient hyperchaotic region and the periodic region are shown in Figs. 5(a) and 5(b), respectively. Note that these phase portraits are hidden attractors.

It is remarkable that the dynamics of system (1) without equilibrium is closely related to the initial states for different control parameters also, which results in that complex transient transition behaviors of hidden attractors occur in system (1). Two examples are illustrated in Figs. 6 and 7, respectively.

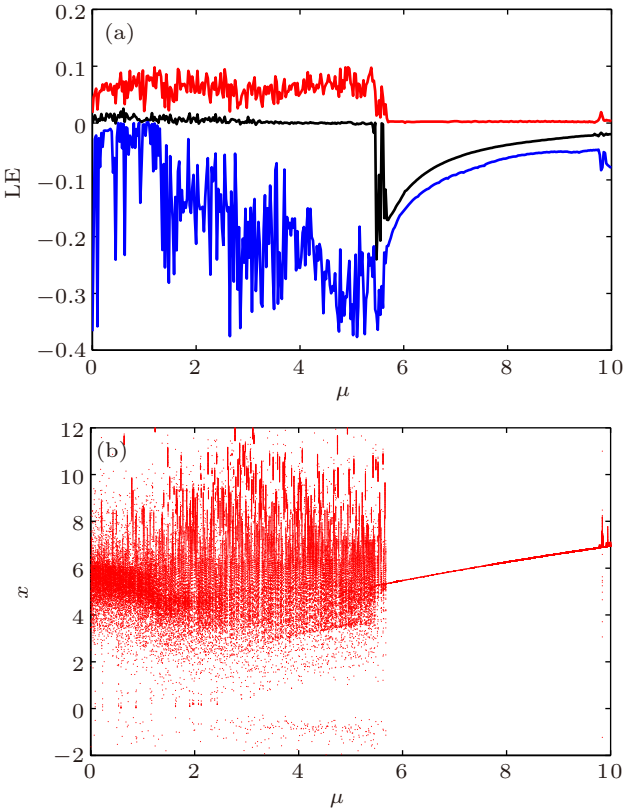


Fig. 4. (color online) Dynamics of the variation of the control parameter μ: (a) largest three Lyapunov exponents; (b) bifurcation diagram of the state variable x.

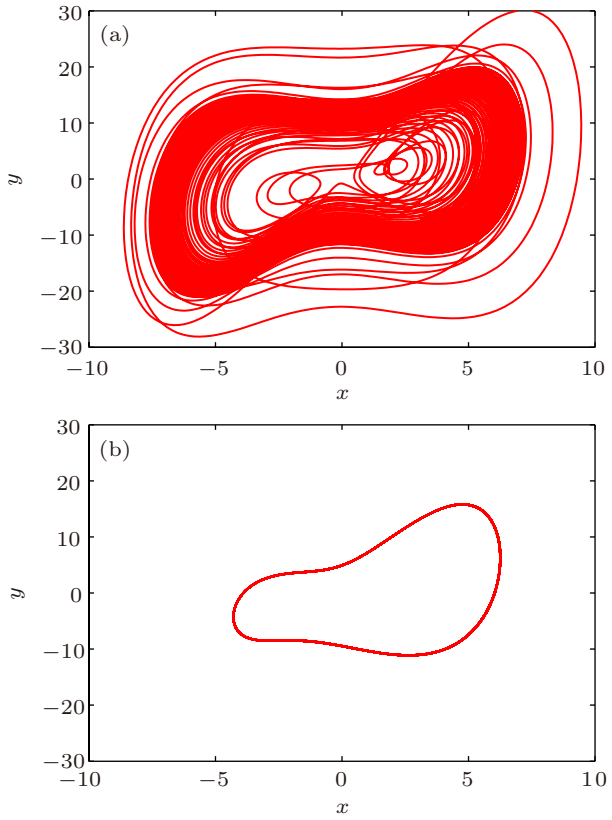


Fig. 5. (color online) Projections on the x–y plane for initial states (1, 1, 1, 1). (a) Transient hyperchaotic attractor at $\mu = 0.52$ with LEs (0.0688, 0.0177, −0.0015, −1.0851). (b) Limit cycle at $\mu = 8$ with LEs (0, −0.0388, −0.0575, −0.9062).

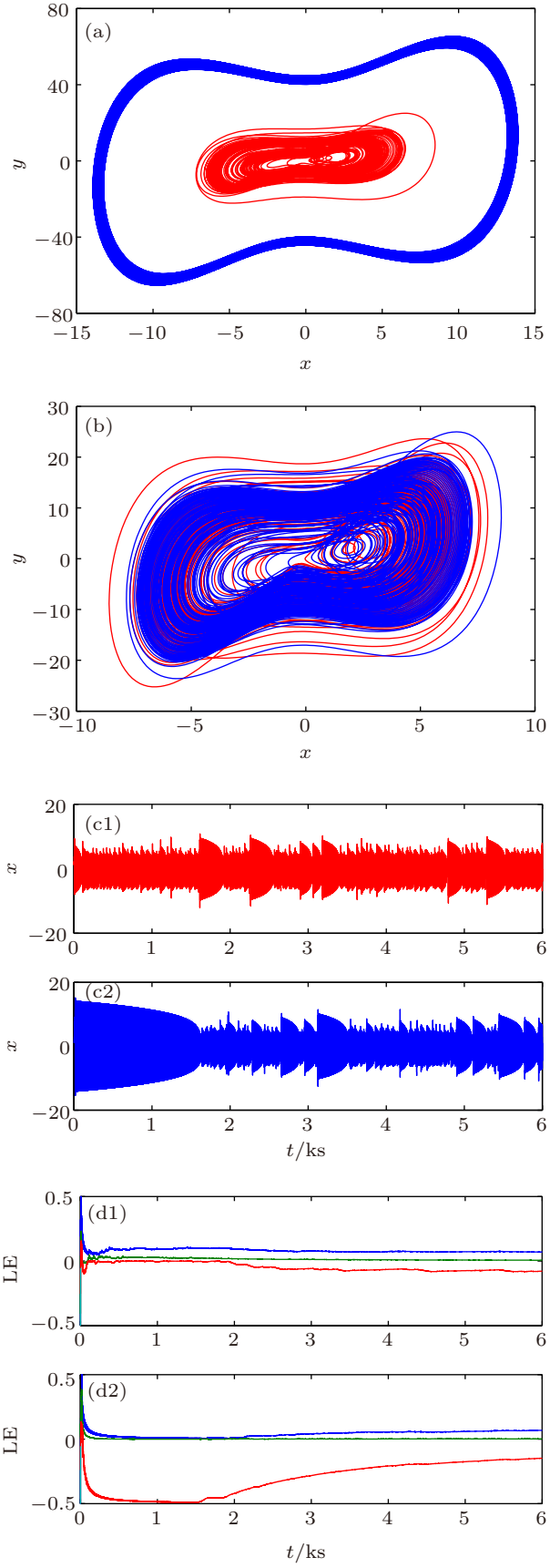


Fig. 6. (color online) Hidden attractors with complex transient behaviors. (a) Projections on the x–y plane in the time interval [100 s, 400 s]. (b) Projections on the x–y plane in the time interval [3.7 ks, 4 ks]. (c) Time-domain waveform of the variable x with different initial states. (d) The largest three Lyapunov exponents against time with different initial states.

When $\mu = 1.5$, the time-domain waveforms, the phase portraits in two different time intervals, and the largest three Lyapunov exponents against the times of two hidden attractors with different initial states are demonstrated in Figs. 6(a), 6(b), 6(c), and 6(d), respectively. In Figs. 6(a), 6(b), and 6(c), the trajectories colored in red start from the initial states (1, 1, 1, 1) and those colored in blue start from the initial states (1, 1, −1, 1); while figures 6(d1) and 6(d2) correspond to the initial states of (1, 1, 1, 1) and (1, 1, −1, 1), respectively.

From Fig. 6, it can be seen that when different initial states are utilized, system (1) has complicated transient transition dynamics. When the initial states are taken as (1, 1, 1, 1), the orbits of system (1) have a transition from transient hyperchaotic to steady chaotic behaviors with the time evolutions; while when the initial states are chosen as (1, 1, −1, 1), the orbits of system (1) have a transition from transient periodic to steady chaotic behaviors with the time evolutions. These complicated transient transition behaviors can be reflected from the Lyapunov exponents against time in Fig. 6(d), where the largest two Lyapunov exponents are greater than zero for the initial states (1, 1, 1, 1) and the largest Lyapunov exponent is close to zero for the initial states (1, 1, −1, 1) during the occurrences of transient transition behaviors, and their four different Lyapunov exponents finally converge to four identical values, respectively.

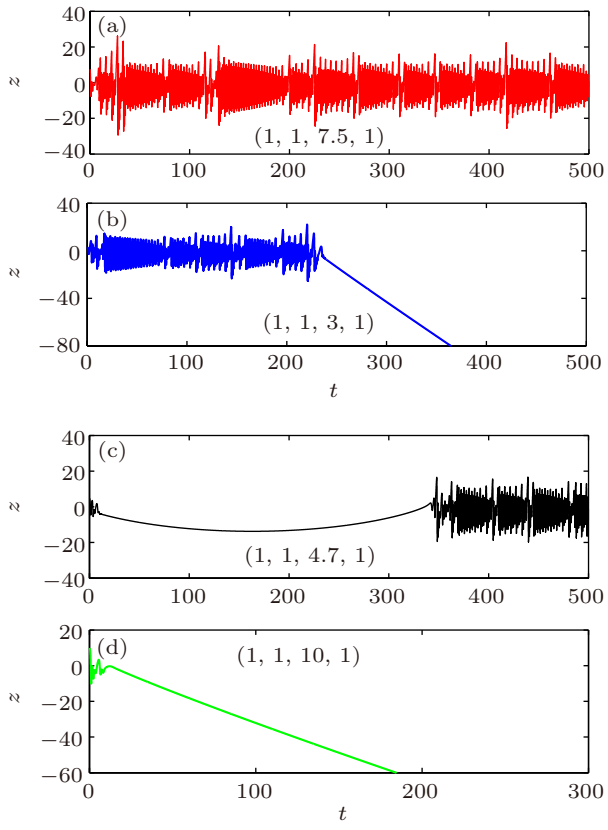


Fig. 7. (color online) Time-domain waveforms of coexisting hidden attractors with different initial states. (a) Steady hyperchaotic behavior. (b) Transient hyperchaotic behavior. (c) Chaotic behavior having long transition time. (d) Unstable sinks.

Figure 7 displays the time-domain waveforms of the state variable z of the coexisting hidden attractors at $\mu = 0.01$. In Fig. 7(a), the initial states and the Lyapunov exponents of system (1) are (1, 1, 7.5, 1) and (0.0617, 0.0204, 0, −1.0826), respectively; in Fig. 7(b), the initial states and the Lyapunov exponents correspond to (1, 1, 3, 1) and (0.0504, 0.0174, 0, −1.0679), respectively; in Fig. 7(c), the initial states and the Lyapunov exponents are equal to (1, 1, 4.7, 1) and (0.0158, 0, −0.4246, −0.5876), respectively; whereas in Fig. 7(d), the initial states and the Lyapunov exponents are equal to (1, 1, 10, 1) and (0.0042, −0.0053, −0.4967, −0.5022), respectively. Observed from Fig. 7, it can be found that the complex transient transition behaviors of the coexisting hidden attractors exist in the proposed system. Note that the above four Lyapunov exponents are the values at $t = 2$ ks.

5. Conclusions

In conclusion, we have studied a simple four-dimensional system with seven terms, two quadratic nonlinearities, and one control parameter. The system has a line equilibrium or no equilibrium resting in the value of the control parameter and exhibits transient hyperchaos, unstable sinks, and hidden attractors over a large parameter region. Especially, the coexisting hidden attractors with complex transient transition behaviors of hyperchaotic attractors, periodic orbits and unstable sinks can be found in the proposed system. The unexpected transient transition behavior is one of the special nonlinear dynamical phenomena which should be avoided in engineering applications.

References

[1] Li C B and Sprott J C 2014 *Int. J. Bifurc. Chaos* **24** 1450034
[2] Zhao H T, Lin Y P and Dai Y X 2014 *Int. J. Bifurc. Chaos* **24** 1450080
[3] Pham V T, Rahma F, Frasca M and Fortuna L 2014 *Int. J. Bifurc. Chaos* **24** 1450087
[4] Jafari S and Sprott J C 2013 *Chaos Soliton. Fract.* **57** 79
[5] Leonov G A, Kuznetsov N V and Vagaitsev V I 2011 *Phys. Lett. A* **375** 2230
[6] Leonov G A, Kuznetsov N V and Vagaitsev V I 2012 *Physica D* **241** 1482
[7] Wei Z and Yang Q 2012 *Nonlinear Dyn.* **68** 543
[8] Wei Z 2011 *Phys. Lett. A* **376** 102
[9] Wang Z, Cang S, Ochola E O and Sun Y 2012 *Nonlinear Dyn.* **69** 531
[10] Stewart I 2000 *Nature* **406** 948
[11] Matsumoto T 1984 *IEEE Trans. Circuits Syst.* **CAS-31** 1055
[12] Lü J H and Chen G R 2002 *Int. J. Bifurc. Chaos* **12** 659
[13] Bao B C, Li C B, Xu J P and Liu Z 2008 *Chin. Phys. B* **17** 4022
[14] Xue W, Qi G Y, Mu J J, Jia H Y and Guo Y L 2013 *Chin. Phys. B* **22** 080504
[15] Bao B C, Xu J P and Liu Z 2010 *Chin. Phys. Lett.* **27** 070504
[16] Li Q D, Zeng H Z and Yang X S 2014 *Nonlinear Dyn.* **77** 255
[17] Leonov G A and Kuznetsov N V 2013 *Int. J. Bifurc. Chaos* **23** 1330002
[18] Leonov G A, Kuznetsov N V, Kiseleva M A, Solovyeva E P and Zaretskiy A M 2014 *Nonlinear Dyn.* **77** 277
[19] Andrievsky B R, Kuznetsov N V, Leonov G A and Pogromsky A Y 2013 *Proc. IFAC* **2013** 75
[20] Li C B and Sprott J C 2014 *Int. J. Bifurc. Chaos* **24** 1450131